

RSC Advances



This is an *Accepted Manuscript*, which has been through the Royal Society of Chemistry peer review process and has been accepted for publication.

Accepted Manuscripts are published online shortly after acceptance, before technical editing, formatting and proof reading. Using this free service, authors can make their results available to the community, in citable form, before we publish the edited article. This *Accepted Manuscript* will be replaced by the edited, formatted and paginated article as soon as this is available.

You can find more information about *Accepted Manuscripts* in the [Information for Authors](#).

Please note that technical editing may introduce minor changes to the text and/or graphics, which may alter content. The journal's standard [Terms & Conditions](#) and the [Ethical guidelines](#) still apply. In no event shall the Royal Society of Chemistry be held responsible for any errors or omissions in this *Accepted Manuscript* or any consequences arising from the use of any information it contains.

A Multivariate Insight into Ionic Liquids Toxicities^{†§}

Alessio Paternò^a, Francesca D'Anna^b, Giuseppe Musumarra^{a*}, Renato Noto^b and Salvatore Scire^a

Abstract

A multivariate insight into Ionic Liquids (ILs) toxicity, a broad term highly dependent on the biological systems adopted as “sensors”, addressed four main groups of toxicities: aquatic toxicity, toxicity towards fungi and bacteria, cytotoxicity towards ICP-81 rat cell lines and acetylcholinesterase enzyme inhibition. This approach, summarizing toxicity information available from a huge amount of scattered literature data, allowed derivation of aquatic toxicity scores for 104 ILs and bacteria and fungi toxicity scores for 87 ILs as well as identification of a correlation between aquatic ecotoxicity and the response of ICP-81 rat cell lines. Further evidence on the effects of cation structural features such as the increase of ILs toxicity on increasing the length of the side chain and its decrease when oxygen atoms are present in the side chain was obtained. Maximum dialkyloxyether imidazolium toxicity was observed for ILs having 7-9 carbon atoms in each side chain, while toxicity decreased for ILs with a higher number of carbons, probably due to the formation of micellar aggregates.

[†]Electronic supplementary information (ESI) available. See DOI:

[§]Dedicated *in memoriam* to Professor Alan R. Katritzky (1928-2014), a worldwide recognised leader of heterocyclic chemistry.

^a Dipartimento di Scienze Chimiche, Università di Catania, Viale A. Doria 6, 95128 Catania, Italy.

^b Dipartimento STEBICEF, Università di Palermo, Viale delle Scienze-Parco d'Orleans II, Ed.17, 90128 Palermo, Italy.

*gmusumarra@unict.it

Introduction

Ionic Liquids (ILs), low melting point salts formed of an organic cation and an inorganic or organic anion, attracted much attention as green solvents due to their low vapour pressure as compared to common volatile organic solvents, resulting in lower air emission, low flammability and non-explosiveness. However these features do not themselves justify their “greenness”.

The increasing number of ILs applications as reaction media,¹⁻⁴ catalysts,⁵⁻⁸ lubricants,⁹ surfactants,¹⁰ anticorrosion agents,^{11,12} in separation science,¹³⁻¹⁶ and more in general in analytical chemistry,¹⁷ prompted several investigations on ILs hazard potential in different biological test systems. Indeed, their water solubility poses the danger of their release and consequently the exertion of negative effects in aquatic ecosystems. On the other hand, high chemical and thermal stability highlight the problem of their bioaccumulation, making the proper assessment of the ionic liquids toxicological profile a problem of major concern.¹⁸

The broad number of combinations of cations and anions determine the chemical properties of ILs as well as their toxicity. Several studies agree that ecotoxicity increases on increasing the side chain hydrophobicity, however many other structural effects may influence eco-sustainability and toxicity. Each of the many publications aimed at the assessment of ILs impact on human's health and environment includes different structures and different aquatic, terrestrial and cell lines models.

Frade and Afonso,¹⁸ who recently provided an overview on the impact of ILs in the environment and in humans, summarized toxicological data for a large number of ILs performed in models of different origin: aquatic toxicity, terrestrial toxicity and toxicological assays aimed at evaluating the impact on humans. This study¹⁸ indicated as a future challenge in the field “to extend the study on aquatic and terrestrial environment to other cations” and “to know whether likely negative impact on water and soil were caused by the same structures as the ones that were showed to be harsher to human and rat cell lines”.

Toxicity data reported in the growing number of studies analyzing the hazard potential for many ionic liquids in different biological test systems were collected and are steadily

updated in a precious database: the UFT-Merck Ionic Liquids Biological Effects Database.¹⁹ The database includes several assays at different levels of biological organization and complexity. These data confirm that ILs have a large “green” potential, but recent studies show that ILs may reveal a low or a high hazard and that the “greenness” strongly depends on the structure.¹⁹

Despite the explosion of ILs applications requires urgently the assessment of their impact on human’s health and environment, each of the available studies investigates different structures and different biological models and an overall picture of ILs toxicity is not available. However, toxicity is a very broad term and tests towards cells and living organism highly depend on the nature of biological systems. Several biological “sensors” have been reported as representative of the hazard of ionic liquids, but a recent review²⁰ points out that available investigations regarding cytotoxicity, toxicity towards invertebrates, vertebrates, fungi and bacteria, phytotoxicity, impact on enzymatic activity and protein stability, provide no simple and uniform picture. Although each “sensor” can be considered as representative of a potential hazard, it is not always available for a wide number of ILs, its determination is affected by specific measurement errors and furthermore different “sensors” can be related to each other providing similar information content. A multivariate approach such as Principal Component Analysis (PCA), applied here for the first time to a data matrix containing experimental measurements of toxicity “sensors” (variables) for a series of ILs (objects), can provide a simplified picture on ILs toxicity. In fact, PCA scores can be determined for a larger set of objects (ILs) with respect to those available for single observables (“sensors”), are affected by lower error as compared to those of single determinations, and summarize the information content into a reduced number of variables (toxicity scales).

In this context aim of the present work is to exploit the potential of multivariate analysis to extract maximum information from the huge amount of scattered available data, herein grouped according to four main kinds of toxicities: (1) aquatic toxicity; (2) toxicity towards fungi and bacteria; (3) cytotoxicity towards ICP-81 rat cell lines; (4) acetyl cholinesterase enzyme inhibition, and to gain a better knowledge on the relationships among them.

Results and Discussion

The UFT database data can be summarized in the form of a Table including 592 structures and 288 measurements (258 biological and 30 degradation tests). In the case of data from different literature sources, values deriving from a higher number of replicates were selected. This Table can be considered as a data matrix where ILs are called objects and biological tests variables. The present investigation would be limited to 451 of the 592 structures, those which have an organic heterocyclic cation. The resulting multivariate data matrix would therefore include 451 ILs (objects) and 258 biological plus 30 degradation tests (variables). However this data matrix has a large number of missing data, therefore we decided to have a multivariate insight by means of PCA by excluding rows and columns from the matrix, in the present case 252 variables and 48 objects (ILs). The remaining 35 variables include biological tests defined as ecotoxicity in the UFT-Merck database herein sub-classified into: aquatic ecotoxicity (e. g. sensitivity to: *Scenedesmus vacuolatus*, *Vibrio fischeri*, *Lemna minor*), toxicity towards fungi and bacteria (e. g. sensitivity to Gram-positive and Gram-negative bacteria and fungi) and toxicity tests on cell viability at a higher level of biological complexity: ICP-81 rat cell lines cytotoxicity and acetylcholinesterase (AChE) enzyme inhibition. The 403 ILs can eventually be analysed as 6 separate classes according to the structure of the heterocyclic cation (imidazolium, piperidinium, morpholinium, pyridinium, pyrrolidinium and quinolinium), and the biological data originally reported as EC₅₀ or IC₅₀ (the concentration at which half of the test organisms or test systems exert a specific effect), MIC (Minimum Inhibitory Concentration) and MBC (Minimum Bactericidal Concentration) were converted into a log scale.

Overall toxicity model

A PCA model from a 403x35 data matrix (ILs in Table S1 and variables in Table S2) provided a 3PC model explaining 85.5% of total variance, where 2 PCs already explain 77% of variance ($Q^2 = 0.587$). The scores plot (Fig. 1), represents the projection of the 403 observations (ILs) from 35 down to two dimensions, i.e. a plane maintaining the most relevant (in the present case 77%) information present in the data set. In this plot no clustering according to the cation can be evidenced. The scores and the loadings plots are

complementary and superimposable, which means that an interesting pattern in the scores plot can be interpreted by looking along the same direction in the loadings plot. In the corresponding loadings plot (Fig.2) all toxicity variables are in the right part of the plot, indicating that the 1st PC is an index of overall toxicity. In Fig. 1 non aromatic rings such as pyrrolidine, piperidine and morpholine appear to be less toxic than aromatic rings (imidazolium, pyridine, quinoline). In agreement with several previous studies, a toxicity increase on increasing alkyl side chain length (i.e. hydrophobicity) can be observed, while the presence of oxygen in the side chain results in lower toxicity for long side chains. No clear cut anion effect can be evidenced in this plot.

The loadings plot in the above overall model (Fig.2) shows also that the 1st PC separates AChE and IPC-81 from all other biological tests, while the 2nd PC is required to discriminate the above two variables. The above finding cannot exclusively be ascribed to their different information content (i.e. they are not representative of ecotoxicity) as the model is somewhat “driven” by the great information content provided by a large number of data for two variables (232 for AChE and 245 for IPC-81) as compared to that of all other variables. This bioinformatics finding has also a rational biological explanation as AChE and IPC-81, biological tests aimed at evaluating toxicity towards more complex living organisms, are expected to have a different information content with respect to the other examined variables. Consequently in order to have a better insight on the influence of the latter variables on ILs ecotoxicity, AChE and IPC-81, were excluded in further PCA analysis and will be considered separately. PCA could not be carried out on a reduced data matrix including both aquatic ecotoxicities and toxicity towards fungi and bacteria as both toxicity data are not available for most ILs, probably due to different hydrophilic/hydrophobic properties which prevent their determination in both systems. Therefore separate PCA models had to be derived for aquatic ecotoxicity and toxicity towards fungi and bacteria.

Aquatic ecotoxicity

PCA was carried out on a 104x6 data matrix (ILs in Table S3 and variables in Table S4), where the variables are aquatic toxicities towards different living organisms: *Scenedesmus vacuolatus* (a green alga), *Vibrio fischeri* (a Gram-negative rod-shaped bacterium found in symbiosis with various marine animals), *Lemna minor* (a floating freshwater aquatic

plant). PCA provided a 2PC model explaining 94.9% of total variance, where the 1st PC already explains 81.1% of variance ($Q^2 = 0.544$). The resulting loadings plot (Fig. 3) shows that the 2nd PC is required to discriminate *Lemna minor* from *Vibrio fischeri* and *Scenedesmus vacuolatus*. The corresponding scores plot (Fig. 4), including mainly imidazolium and pyridinium cations, opens a two dimensional window into ILs aquatic toxicity. This plot shows that the different nature of aromatic cations has not a significant effect on toxicity (although non aromatic heterocycles such as pyrrolidine, piperidine and morpholine appear to be less toxic) and no significant anion effect can be evidenced. The first PC score can be assumed as an estimate of aquatic toxicity with less toxic ILs in the right part of the plot and more toxic ones on the left. The first PC scores, which can be considered as a unique “aquatic ecotoxicity score” for all the examined 104 ILs, are reported in Table 1 in order of decreasing t_1 values corresponding to increasing toxicity, together with the rank of the same ILs in Table S5 (logICP-81 rat cell lines growth inhibition) and S6 (log AChE enzyme inhibition) respectively. Comparison with the latter values will be discussed later in the section: Relationships between different toxicities.

The procedure adopted here to derive the above toxicity scores is not new and it is analogous to that already adopted to parameterise discrete variables (solvent, catalyst, etc.) by means of the so-called “principal properties” (PP), quantitative descriptors presently available for Lewis acids,²¹ amines,²¹ ketones,²¹ aromatic substituents,²² amino acids,²³⁻²⁵ heteroaromatics,^{26,27} solvents^{21,28} and lanthanide triflates.²⁹ PPs are the scores of a PCA analysis applied to a data matrix containing a series of experimental observations (variables) for a set of chemical structures (objects) and are suitable for experimental design as they are orthogonal to each other. Other advantages are that they can be determined for a larger set of objects with respect to those available for single observables in the matrix and are affected by lower errors as compared to those of the single observables determinations as PCA derives them exploiting similar information content provided by the original variables. It is worth mentioning here that no single aquatic toxicity test is available for such a high number of ILs (104) and that this result could be achieved by applying multivariate data analysis to six different tests, each available for a lower number of ILs.

Toxicity towards fungi and bacteria

PCA was carried out on an 87x26 data matrix (ILs in Table S7 and variables in Table S8), where the variables are 26 non-aquatic toxicities. PCA provided a 7PC model explaining 96.2% of total variance, where 3 PCs explain 86.7% of variance ($Q^2 = 0.728$) and the 1st PC explains already 70.4% of variance ($Q^2 = 0.66$). The p_2 - p_3 loadings plot (Figure 5) shows that the 2nd and 3rd components (both of which are statistically significant and explain only a further 16.3% of variance as compared to the 1st PC) are required to discriminate the variables into Gram-positive bacteria (in the lower left quadrant), Gram-negative bacteria (in the two right quadrants), and fungi (in the upper left quadrant). This finding points out the potentialities of PCA, a totally independent numerical data analysis, in recognising different groups according to a well known microbiological classification. However, the most relevant information provided in all 26 tests is summarized by the 1st PC explaining above 70% of variance. Therefore the first PC scores can again be assumed as an estimate of ILs toxicity towards fungi and bacteria with less toxic ILs exhibiting a high t_1 value. In the t_1 - t_2 scores plot (Fig.6) only 3 cations (imidazolium, pyridinium and quinolinium) are present (due to the lack of experimental data for the others) and exhibit t_1 values distributed all over the 1st PC.

The first PC scores, which can be defined as “toxicity towards fungi and bacteria scores” for all the examined 87 ILs are reported in Table 2 in order of decreasing t_1 values, i.e. of increasing toxicity. It is worth mentioning that none of the 26 fungi and bacteria toxicities in the matrix was available for as many as 87 ILs and that the above scores are affected by lower errors as compared to single toxicity determinations and comprise information provided by both Gram-positive and Gram-negative bacteria as well as by fungi.

Imidazolium cations model

In previous sections, where PC models were obtained for ILs containing six different heterocyclic cations, no clear cut anion effects could be evidenced. The selection of the data matrices for PCA is limited by the data structure depending on the abundance of available data, therefore decisions on how to improve the model quality for specific purposes at the expense of generality are subjective choices guided by the information provided by PCA as the investigation goes along.

In order to achieve a deeper insight into the effect of anions, PCA was limited to imidazolium cations (a data matrix with 218 ILs and 43 biological and degradation tests). In this case PCA provided a 3PC model explaining 85% of total variance ($Q^2 = 0.706$) with the 1st PC explaining already 66% of variance ($Q^2 = 0.594$).

In the t_1 - t_2 scores plot reported in Fig. 7, where ILs are coloured according to the anion, no clustering of anions can be observed, pointing out that the anion has not a key role in addressing the ILs toxicity, which appears more significantly affected by the chemical structure of the imidazolium substituents. These effects can be better evidenced by carrying out a PCA on a data matrix including only ILs with the same cation scaffold (imidazolium) and the same anion (chloride). This data matrix contains 37 ILs and 24 biological and degradation tests. The t_1 - t_2 scores plot (Fig. 8) shows in the right part of the plot (less toxic compounds according to superimposition with the p_1 - p_2 loadings reported in Fig. 9) ILs with short alkyl side chains and dialkyloxyethers with short (2-5) and long (11-14) carbon alkyl chains, whereas ILs with long alkyl side chains and dialkyloxyethers with medium length (7-10 carbon atoms) can be found in the left part of the plot (toxic compounds). The higher toxicity of alkyylimidazolium with longer side chains is well known and has been reported in the literature also for pyrrolidinium, piperidinium and pyridinium ILs and related to the higher hydrophobicity of long side chains.²⁰ However, the toxicity “levelled off on reaching a threshold side chain length”²⁰ which depends on the IL class. It has also been noted that “the presence of oxygen in the side chain seems to decrease the toxicity”.²⁰ Pernak et al.³⁰ reported that mono alkyloxyether imidazoliums exhibit a maximum of toxicity (microbial toxicity) for dodecyloxymethyl imidazolium (12 carbon atom side chain), while a toxicity decrease was observed up to 16 carbon atoms side chains. Garcia et al.³¹ recently reported an analogous behavior for monoalkylesters imidazolium and pyridinium ILs. They noted that an increase of the carbon atoms in the ester side chain resulted in a higher tendency to form micellar aggregates. In this context we can observe (Figure 8) high toxicity of dialkyloxyether imidazoliums for ILs having 7-9 carbon atoms in each side chain. The decrease of toxicity observed for dialkyloxyethers ILs with more than 12 carbon atoms in each side chain may be ascribed to the formation of micellar aggregates, which avoid the interaction of the ILs with the cell membrane.³¹ Therefore toxicity might be due to a balance of hydrophobicity and formation of micelles. The above toxicity trend found for the overall imidazolium model has been confirmed in

the case of more specific models which consider separately toxicity towards aquatic organisms and towards fungi and bacteria. (Figures S9 and S10 in SI).

Relationships between different toxicities

One of the aims of the present study is to assess if a negative impact on water can be ascribed to the same structures as the ones that were showed to be harsher to rat cell lines and humans such as IPC-81 and AChE inhibition respectively. Estimation of the latter toxicities by PCA, Neural Network (NN) and multilayer perceptron has been reported.³²

In Tables S5 and S6 we report respectively the log of ICP-81 rat cell lines growth inhibition, and AChE enzyme inhibition ordered according to decreasing values, i.e. of increasing toxicity. Figure 10a shows no correlation between the latter toxicity measurements, as expected on the basis of the biological differences in these toxicity “sensors”. It is worth to comment also correlations between the t_1 scores of the aquatic ecotoxicity model and IPC-81 and AChE values plotted in Figures 10b and 10c. No correlation can be observed with the enzymatic activity (Fig. 10b), while a correlation with IPC-81 can be envisaged (Fig. 10c). The latter correlation provides an answer to the question whether “a negative impact on water” may be “caused by the same structures as the ones that were showed to be harsher to rat cell lines”.¹⁸ In fact the impact of aquatic ecotoxicity is found to be paralleled by an effect on the cellular response in living organisms such as ICP-81 rat cell lines. IPC-81 and AChE toxicity values are not available for most ILs tested with fungi and bacteria, therefore no correlation can be attempted with t_1 scores of this model.

Table 1 reports the ILs according to the aquatic toxicity t_1 “scores” together with the rank of the same ILs in Tables S5 (log ICP-81 rat cell lines growth inhibition) and S6 (log AChE enzyme inhibition) respectively. According to three out of the four toxicities considered in the present work, compounds n. 2, 4, 7, 8, 12, 17 and 20 (Chart 1) can be recommended as safe ILs, while the use of 86, 87, 93, 96, 101, 103 and 104 (Chart 2) should be discouraged or limited, provided that appropriate actions are taken, to cases in which no task specific applicative alternatives are available. The latter ILs should be assigned priority in more extensive (and more expensive) toxicological studies. Guidance on the choice of less toxic ILs according to fungi and bacteria ecotoxicity (the fourth kind of toxicity considered in the present work) can be obtained from Table 2. Inspection of

both Tables 1 and 2 is necessary to obtain information about ILs toxicity, as it was not possible to summarize available toxicity information using a unique toxicity score, due to the lack of data which can be ascribed to different ILs hydrophilic/hydrophobic properties preventing their determination in different biological “sensors”. However, the above tables provide a simplified picture of scattered toxicity data available in the literature very useful for the new EU chemical legislation for the Registration, Evaluation, Authorisation and Restriction of Chemicals (REACH) adopted in June 2007.

Conclusions

A multivariate insight into ILs toxicity, a broad term highly dependent on the biological systems adopted as “sensors”, achieved these goals in relation to the aims of the study:

1. Derivation of consistent toxicity “scores” for aquatic and bacteria and fungi toxicities (now available for an unprecedented significant number of ILs) summarizing toxicity information available from a huge amount of scattered literature data regarding specific biological “sensors”.
2. Estimation of quantitative relationships among different toxicities evidencing a correlation between aquatic ecotoxicity and the response of ICP-81 rat cell lines.
3. Confirmation of the effects of cation structural features such as the increase of ILs toxicity on increasing the length of the side chain, its decrease when oxygen atoms are present in the side chain, and the presence of a maximum of toxicity for a given side chain length depending on the specific cationic moiety, which may be ascribed to the formation of micellar aggregates.

Evaluation of the negative impact of ILs on water and soil, as well as on rat and human cell lines, is a complicated task. The present work, providing a comprehensive picture and guidelines for the evaluation of ILs toxicity, paves the way towards a rational selection of eco-sustainable ILs for specific applications. Of course the destination is far from being reached. However, a better knowledge on the quantitative relationships between the chemical structures of ILs, their physicochemical properties, and their biological activities would move a step forward in the right direction. Investigations in this context are in progress in our laboratories.

Statistical Methods

In the present work, the PCA procedure was carried out by means of the SIMCA software package (SIMCA 13.0.3, Umetrics, Umea, Sweden) using data matrices obtained from data available on the web in a database collected by Merck (UFT-Merck Ionic Liquids Biological Effects Database).¹⁹

The data were pre-processed by autoscaling all variables to unitary variance, i.e. by multiplying the variables by appropriate weights (the reciprocal of the variable standard deviation) to give them unit variance (i.e. the same importance). Autoscaled matrix elements were then fitted into a model given by equation (1), where the number A of significant cross terms (components), and the parameters p_{ak} and t_{ia} are calculated by minimising the residuals e_{ik} , after subtracting \bar{x}_k (the mean value of the i^{th} experimental quantities x_k).

$$x_{ik} = \bar{x}_k + \sum_{a=1}^{a=A} t_{ia} p_{ak} + e_{ik} \quad (1)$$

Parameters \bar{x}_k and p_{ak} (the loadings) depend only on the variables, and the t_{ia} (scores) only on the objects. The deviations from the model are expressed by the residuals e_{ik} . The number of significant components (A) was determined using the cross-validation (CV) technique.³³ CV was performed by dividing the data into a number of groups (five to nine) and then developing a number of parallel models from reduced data with one of the groups deleted. The performance of the model can be evaluated by two parameters: R^2 related to the goodness of fit and Q^2 to the goodness of prediction.

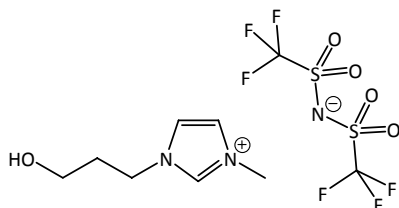
Acknowledgements

We thank the University of Catania for a PhD grant (to AP).

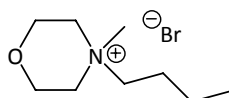
References

- 1 R. Mancuso, C. S. Pomelli, C. Chiappe, R. C. Larock and B. Gabriele, *Org. Biomol. Chem.*, 2014, **12**, 651-659.
- 2 N. Szesni, K. Meyer and P. Wasserscheid, *ChemCatChem*, 2014, **6**, 162-169.
- 3 F. D'Anna, S. Marullo, P. Vitale and R. Noto, *Ultrason. Sonochem.*, 2012, **19**, 136-142.
- 4 E. E. L. Tanner, R. R. Hawker, H. M. Yau, A. K. Croft and J. B. Harper, *Org. Biomol. Chem.*, 2013, **11**, 7516-7521.
- 5 A. Forsyth, U. Frohlich, P. Goodrich, H. Q. N. Gunaratne, C. Hardacre, A. McKeown and K. R. Seddon, *New J. Chem.*, 2010, **34**, 723-731.
- 6 C. S. Consorti, G. L. P. Aydos and J. Dupont, *Chem. Commun.*, 2010, **46**, 9058-9060.
- 7 F. D'Anna, S. Marullo, P. Vitale and R. Noto, *Eur. J. Org. Chem.*, 2011, **2011**, 5681-5689.
- 8 F. D'Anna, S. Marullo and R. Noto, *J. Org. Chem.*, 2008, **73**, 6224-6228.
- 9 A. E. Somers, B. Khemchandani, P. C. Howlett, J. Sun, D. R. MacFarlane and M. Forsyth, *ACS Appl. Mater. Interfaces*, 2013, **5**, 11544-11553.
- 10 Z. Liu, P. Hu, X. Meng, R. Zhang, H. Yue, C. Xu and Y. Hu, *Chem. Eng. Sci.*, 2014, **108**, 176-182.
- 11 P. K. Khatri, G. D. Thakre and S. L. Jain, *Ind. Eng. Chem. Res.*, 2013, **52**, 15829-15837.
- 12 Q. Zhang, Q. Wang, S. Zhang and X. Lu, *J. Solid State Electrochem.*, 2014, **18**, 257-267.
- 13 S. Rodríguez-Sánchez, P. Galindo-Iranzo, A. C. Soria, M. L. Sanz, J. E. Quintanilla-López and R. Lebrón-Aguilar, *J. Chromatogr. A*, 2014, **1326**, 96-102.
- 14 S. Hyvärinen, J. P. Mikkola, D. Y. Murzin, M. Vaheer, M. Kaljurand and M. Koel, *Catalysis Today*, 2014, **223**, 18-24.
- 15 M. D. Joshi, J. L. Anderson, *RSC Advances*, 2012, **2**, 5470-5484.
- 16 L. Vidal, M. L. Riekkola, A. Canals, *Anal. Chim. Acta*, 2012, **715**, 19-41.
- 17 T. D. Ho, C. Zhang, L.W. Hantao, J. L. Anderson, *Anal. Chem.*, 2014, **86**, 262-285.
- 18 R. F. M. Frade and C. A. M. Afonso, *Hum. Exp. Toxicol.*, 2010, **29**, 1038-1054.
- 19 UFT-Merck Ionic Liquids Biological Effects Database: <http://www.il-eco.uft.uni-bremen.de/> (accessed October 2013).
- 20 K. S. Egorova and V. P. Ananikov, *ChemSusChem*, 2014, **7**, 336-360.
- 21 R. Carlson and J. E. Carlson, *Design and optimization in organic synthesis. Second revised and enlarged edition*, Amsterdam, Elsevier, 2005.
- 22 M. Skagerberg, D. Bonelli, S. Clementi, G. Cruciani and C. Ebert, *Quant. Struct.-Act. Relat.*, 1989, **8**, 32-38.
- 23 S. Hellberg, M. Sjöström, and S. Wold, *Acta Chem. Scand.*, 1986, **B40**, 135-140.
- 24 S. Hellberg, M. Sjöström, B. Skagerberg and S. Wold, *J. Med. Chem.*, 1987, **30**, 1127-1135.
- 25 M. Skagerberg, M. Sjöström and S. Wold, *J. Chemometrics*, 1990, **4**, 241-253.
- 26 G. Caruso, G. Musumarra and A. R. Katritzky, *Quant. Struct.-Act. Rel.*, 1993, **12**, 146-151.
- 27 S. Clementi, G. Cruciani, D. Riganelli, R. Valigi and G. Musumarra, *Quant. Struct.-Act. Rel.*, 1996, **15**, 108-120.

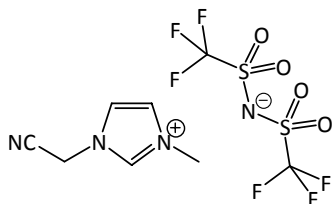
- 28 F. P. Ballistreri, C. G. Fortuna, G. Musumarra, D. Pavone and S. Scirè, *Arkivoc*, 2002, **part (xi)**, 54-56 or at <http://arkat-usa.org/ark/journal/2002/Spinelli/MS-568H/568H.htm>.
- 29 C. G. Fortuna, G. Musumarra, M. Nardi, A. Procopio, G. Sindona, and S. Scirè, *J. Chemometrics*, 2006, **20**, 418-424.
- 30 J. Pernak, K. Sobaszekiewicz and I. Mirska, *Green Chemistry*, 2003, **5**, 52-56.
- 31 M. T. Garcia, I. Ribosa, L. Perez, A. Manresa and F. Comelles, *Langmuir*, 2013, **29**, 2536-2545.
- 32 J. S. Torrecilla, J. Garcia, E. Rojo and F. Rodríguez, *J.Hazard. Mater.*, 2009, **164**, 182-194.
- 33 S. Wold, *Technometrics*, 1978, **20**, 397-405.

Chart 1: Eco- and biosustainable ILs

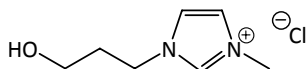
1-(3-Hydroxypropyl)-3-methylimidazolium 1,1,1-trifluoro-N-[(trifluoromethyl)sulfonyl]methanesulfonamide



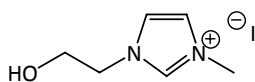
4-Butyl-4-methylmorpholinium bromide



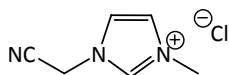
1-(Cyanomethyl)-3-methylimidazolium 1,1,1-trifluoro-N-[(trifluoromethyl)sulfonyl]methanesulfonamide



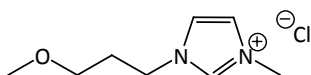
1-(3-Hydroxypropyl)-3-methylimidazolium chloride



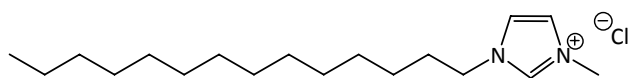
1-(2-Hydroxyethyl)-3-methylimidazolium iodide



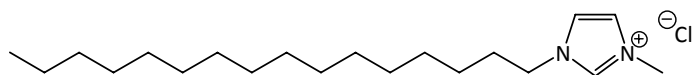
1-(Cyanomethyl)-3-methylimidazolium chloride



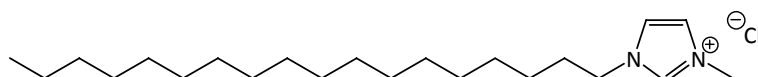
1-(3-Methoxypropyl)-3-methylimidazolium chloride

Chart 2: Potentially toxic ILs

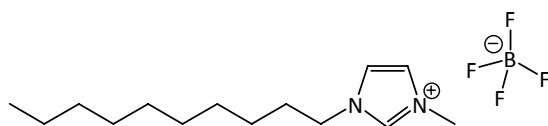
1-Methyl-3-tetradecylimidazolium chloride



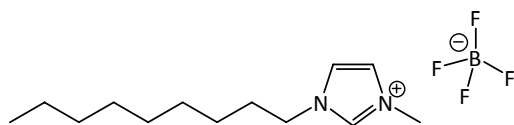
1-Hexadecyl-3-methylimidazolium chloride



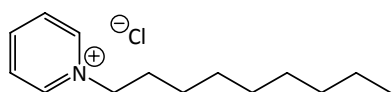
1-Methyl-3-octadecylimidazolium chloride



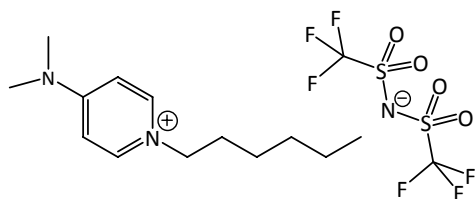
1-Decyl-3-methylimidazolium tetrafluoroborate



1-Methyl-3-nonylimidazolium tetrafluoroborate



1-Octylpyridinium chloride



4-(Dimethylamino)-1-hexylpyridinium 1,1,1-trifluoro-N-[(trifluoromethyl)sulfonyl]methanesulfonamide

Table 1: Ranking of ILs according to Aquatic toxicity model together with IPC-81 toxicity rank and AChE toxicity rank.

	CAS no.	Name	t[1] Aquatic toxicity model	IPC-81 Rank ^a	AChE Rank ^b
1	174899-81-1	1,3-Dimethylimidazolium 1,1,1-trifluoro-N-[(trifluoromethyl)sulfonyl]methanesulfonamide	3,91		
2	827027-30-5	1-(3-Hydroxypropyl)-3-methylimidazolium 1,1,1-trifluoro-N-[(trifluoromethyl)sulfonyl]methanesulfonamide	3,24	61	22
3	342573-75-5	1-Ethyl-3-methylimidazolium ethyl sulfate	3,21	57	117
4	75174-77-5	4-Butyl-4-methylmorpholinium bromide	3,18	17	50
5	none (2013-09-19)	1-Methyl-1-propylpiperidinium hexafluorophosphate	2,90		
6	216300-12-8	1-Methyl-3-propylimidazolium hexafluorophosphate	2,89	155	88
7	937720-90-6	1-(Cyanomethyl)-3-methylimidazolium 1,1,1-trifluoro-N-[(trifluoromethyl)sulfonyl]methanesulfonamide	2,73	36	14
8	355011-34-6	1-(3-Hydroxypropyl)-3-methylimidazolium chloride	2,62	28	33
9	342789-81-5	1-Butyl-3-methylimidazolium methanesulfonate	2,61	101	138
10	94280-72-5	1-Butyl-1-methylpiperidinium bromide	2,44	46	171
11	945996-02-1	1-(Ethoxymethyl)-3-methylimidazolium chloride	2,38	104	65
12	1012794-00-1	1-(2-Hydroxyethyl)-3-methylimidazolium iodide	2,15	15	21
13	410522-18-8	1-Butyl-3-methylimidazolium 4-methylbenzenesulfonate	2,01	118	112
14	448245-52-1	1-Butyl-3-methylimidazolium N-cyanocyanamide	1,97	152	166
15	85100-77-2	1-Butyl-3-methylimidazolium bromide	1,92	121	152
16	608140-12-1	1-Methyl-1-propylpiperidinium 1,1,1-trifluoro-N-[(trifluoromethyl)sulfonyl]methanesulfonamide	1,78	119	
17	154312-63-7	1-(Cyanomethyl)-3-methylimidazolium chloride	1,54	38	49
18	874-80-6	1-Butylpyridinium bromide	1,44	67	181
19	324574-95-0	4-Butyl-4-methylmorpholinium 1,1,1-trifluoro-N-[(trifluoromethyl)sulfonyl]methanesulfonamide	1,44	80	17
20	1012794-06-7	1-(3-Methoxypropyl)-3-methylimidazolium chloride	1,38	9	63
21	827027-29-2	1-(3-Hydroxypropyl)pyridinium 1,1,1-trifluoro-N-[(trifluoromethyl)sulfonyl]methanesulfonamide	1,33	73	40
22	none (2013-09-19)	1-Methyl-3-(2-methylpropyl)imidazolium 1,1,1-trifluoro-N-[(trifluoromethyl)sulfonyl]methanesulfonamide	1,32		
23	1015254-36-0	1-(3-Methoxypropyl)-3-methylimidazolium 1,1,1-trifluoro-N-[(trifluoromethyl)sulfonyl]methanesulfonamide	1,29	88	35
24	216299-72-8	1-Methyl-3-propylimidazolium 1,1,1-trifluoro-N-[(trifluoromethyl)sulfonyl]methanesulfonamide	1,25		
25	460983-97-5	1-Hexylpyridinium 1,1,1-trifluoro-N-[(trifluoromethyl)sulfonyl]methanesulfonamide	1,25	144	109
26	1332694-08-2	1-(3-Hydroxypropyl)-1-methylpyrrolidinium 1,1,1-trifluoro-N-[(trifluoromethyl)sulfonyl]methanesulfonamide	1,22	68	19
27	1241842-94-3	1-[1-(1,3-Benzodioxol-5-yl)-2-methoxy-2-oxoethyl]pyridinium bromide	1,22		
28	1049751-90-7	4-(Ethoxymethyl)-4-methylmorpholinium 1,1,1-trifluoro-N-[(trifluoromethyl)sulfonyl]methanesulfonamide	1,22	82	11
29	827033-71-6	1-Butylpyridinium N-cyanocyanamide	1,21		
30	479500-35-1	1-Butyl-1-methylpyrrolidinium chloride	1,11	26	175
31	174899-88-8	1,3-Diethylimidazolium 1,1,1-trifluoro-N-[(trifluoromethyl)sulfonyl]methanesulfonamide	1,04		
32	129412-64-2	1-(2-Ethoxy-2-oxoethyl)-1-methylpyrrolidinium bromide	1,03	66	
33	65039-09-0	1-Ethyl-3-methylimidazolium chloride	1,00	74	164
34	623580-02-9	1-Butyl-1-methylpiperidinium 1,1,1-trifluoro-N-[(trifluoromethyl)sulfonyl]methanesulfonamide	0,97	84	122

35	244193-49-5	1-Methyl-3-pentylimidazolium tetrafluoroborate	0,94	162	167
36	244193-48-4	1-Methyl-3-propylimidazolium tetrafluoroborate	0,92	117	93
37	474972-46-8	1-(2-Methoxyethyl)-3-methylimidazolium chloride	0,88	27	68
38	174899-82-2	1-Ethyl-3-methylimidazolium 1,1,1-trifluoro-N-[(trifluoromethyl)sulfonyl]methanesulfonamide	0,87	95	90
39	1012793-99-5	1-(2-Ethoxyethyl)-3-methylimidazolium bromide	0,77	34	89
40	178631-01-1	1-(2-Methoxyethyl)-3-methylimidazolium 1,1,1-trifluoro-N-[(trifluoromethyl)sulfonyl]methanesulfonamide	0,73	102	46
41	65039-05-6	1-Butyl-3-methylimidazolium iodide	0,64	97	118
42	370865-89-7	1-Ethyl-3-methylimidazolium N-cyanocyanamide	0,60	81	74
43	1107545-20-9	1-(2-Ethoxy-2-oxoethyl)-1-methylpyrrolidinium 1,1,1-trifluoro-N-[(trifluoromethyl)sulfonyl]methanesulfonamide	0,49	64	5
44	742099-80-5	1-Ethyl-3-methylimidazolium tetracyanoborate	0,46	103	144
45	945996-13-4	1-(Ethoxymethyl)-3-methylimidazolium 1,1,1-trifluoro-N-[(trifluoromethyl)sulfonyl]methanesulfonamide	0,46	108	51
46	757240-24-7	1-(2-Methoxyethyl)-1-methylpyrrolidinium 1,1,1-trifluoro-N-[(trifluoromethyl)sulfonyl]methanesulfonamide	0,31	93	79
47	79917-90-1	1-Butyl-3-methylimidazolium chloride	0,27	114	176
48	666823-18-3	1-Ethyl-3-methylimidazolium, salt with methanetricarbonitrile (1:1)	0,24	140	67
49	67226-45-3	1-Butylpyridinium μ -chlorohexachlorodialuminate	0,23	71	150
50	none (2013-09-19)	1-Butyl-3-methylimidazolium hexafluorophosphate	0,21	143	94
51	26576-85-2	1-Butyl-3-methylpyridinium bromide	0,21		
52	1049751-95-2	1-(3-Methoxypropyl)-1-methylpiperidinium 1,1,1-trifluoro-N-[(trifluoromethyl)sulfonyl]methanesulfonamide	0,21	94	62
53	663628-46-4	1-(2-Ethoxyethyl)-1-methylpyrrolidinium 1,1,1-trifluoro-N-[(trifluoromethyl)sulfonyl]methanesulfonamide	0,18	106	39
54	244193-50-8	1-Hexyl-3-methylimidazolium tetrafluoroborate	0,15	161	156
55	26576-98-7	1-Butyl-3,5-dimethylpyridinium bromide	0,13		
56	1124-64-7	1-Butylpyridinium chloride	0,09		189
57	174899-83-3	1-Butyl-3-methylimidazolium 1,1,1-trifluoro-N-[(trifluoromethyl)sulfonyl]methanesulfonamide	0,02	170	95
58	712355-12-9	1-Butyl-3-methylpyridinium N-cyanocyanamide	-0,04	115	208
59	174501-65-6	1-Butyl-3-methylimidazolium tetrafluoroborate	-0,06	151	143
60	710336-91-7	1-Butyl-3-methylimidazolium 1,1,1-trifluoro-N-(trifluoromethyl)methanamine	-0,06	201	183
61	343952-33-0	1-Butyl-4-methylpyridinium tetrafluoroborate	-0,07	163	190
62	1241842-26-1	1-[1-(1,3-Benzodioxol-5-yl)-2-butoxy-2-oxoethyl]-3-methylimidazolium bromide	-0,08		
63	350493-08-2	1-Butyl-2,3-dimethylimidazolium 1,1,1-trifluoro-N-[(trifluoromethyl)sulfonyl]methanesulfonamide	-0,16		
64	174899-66-2	1-Butyl-3-methylimidazolium trifluoromethanesulfonate	-0,19	148	131
65	347882-21-7	1-Ethyl-3-propylimidazolium 1,1,1-trifluoro-N-[(trifluoromethyl)sulfonyl]methanesulfonamide	-0,20		
66	852616-00-3	1-Ethyl-3-methylimidazolium bis(pentafluoroethyl)phosphinate	-0,21	154	83
67	697248-62-7	1-Hexyl-3-methylimidazolium, salt with 1,2-benzisothiazol-3(2H)-one 1,1-dioxide (1:1)	-0,28	193	108
68	778593-17-2	1-(2-Ethoxyethyl)-3-methylimidazolium 1,1,1-trifluoro-N-[(trifluoromethyl)sulfonyl]methanesulfonamide	-0,28	72	76
69	1424967-13-4	1-[1-(1,3-Benzodioxol-5-yl)-2-butoxy-2-oxoethyl]pyridinium bromide	-0,41		
70	380497-19-8	1-Hexyl-1-methylpyrrolidinium 1,1,1-trifluoro-N-[(trifluoromethyl)sulfonyl]methanesulfonamide	-0,48	177	30
71	1241840-01-6	1-[1-(3,4-Dimethoxyphenyl)-2-methoxy-2-oxoethyl]pyridinium chloride	-0,49		
72	877678-54-1	1-Butyl-3,5-dimethylpyridinium N-cyanocyanamide	-0,54		
73	244193-51-9	1-Heptyl-3-methylimidazolium tetrafluoroborate	-0,66	184	101
74	1241842-81-8	1-[1-(1,3-Benzodioxol-5-yl)-2-methoxy-2-oxoethyl]-3-methylimidazolium chloride	-0,69		

75	749921-07-1	1,3-Dibutylimidazolium 1,1,1-trifluoro-N-[(trifluoromethyl)sulfonyl]methanesulfonamide	-0,71		
76	445473-58-5	1-Butyl-3-methylimidazolium octylsulfate	-0,89	120	103
77	393550-29-3	1-Ethyl-3-hexylimidazolium tetrafluoroborate	-1,00	200	158
78	376650-04-3	1-Ethyl-3-methylimidazolium bis[1,2-benzenediolato(2-)-O1,O2]borate	-1,06	231	92
79	67021-56-1	1-Hexyl-3-methylpyridinium bromide	-1,08		
80	280779-53-5	1-Methyl-3-pentylimidazolium 1,1,1-trifluoro-N-[(trifluoromethyl)sulfonyl]methanesulfonamide	-1,16		
81	none (2013-09-19)	1,3-Dipropylimidazolium 1,1,1-trifluoro-N-[(trifluoromethyl)sulfonyl]methanesulfonamide	-1,21		
82	none (2013-09-19)	1,3-Dihexylimidazolium 1,1,1-trifluoro-N-[(trifluoromethyl)sulfonyl]methanesulfonamide	-1,21		
83	474972-49-1	1-[2-(2-Methoxyethoxy)ethyl]-3-methylimidazolium chloride	-1,42		
84	304680-35-1	1-Hexyl-3-methylimidazolium hexafluorophosphate	-1,54	159	136
85	171058-17-6	1-Hexyl-3-methylimidazolium chloride	-1,57	180	169
86	872672-57-6	4-(Dimethylamino)-1-hexylpyridinium 1,1,1-trifluoro-N-[(trifluoromethyl)sulfonyl]methanesulfonamide	-1,57	227	212
87	4086-73-1	1-Octylpyridinium chloride	-1,59	228	188
88	none (2013-09-19)	1,3-Dipentylimidazolium 1,1,1-trifluoro-N-[(trifluoromethyl)sulfonyl]methanesulfonamide	-1,74		
89	1241842-28-3	1-[2-[1-(1,3-Benzodioxol-5-yl)-2-butoxy-2-oxoethoxy]-2-oxoethyl]-3-methylimidazolium bromide	-1,96		
90	1241839-96-2	1-[2-[1-(1,3-Benzodioxol-5-yl)-2-methoxy-2-oxoethoxy]-2-oxoethyl]pyridinium bromide	-2,13		
91	425382-14-5	1-Heptyl-3-methylimidazolium 1,1,1-trifluoro-N-[(trifluoromethyl)sulfonyl]methanesulfonamide	-2,13		
92	85100-78-3	1-Hexyl-3-methylimidazolium bromide	-2,43		
93	244193-55-3	1-Methyl-3-nonylimidazolium tetrafluoroborate	-2,57	217	192
94	382150-50-7	1-Hexyl-3-methylimidazolium 1,1,1-trifluoro-N-[(trifluoromethyl)sulfonyl]methanesulfonamide	-2,86	191	71
95	872672-72-5	3-Methyl-1-octylpyridinium bromide	-3,56		
96	244193-56-4	1-Decyl-3-methylimidazolium tetrafluoroborate	-3,56	233	205
97	878005-11-9	1-Ethyl-3-methylimidazolium trifluorotris(pentafluoroethyl)phosphate	-3,60	226	43
98	178631-04-4	1-Methyl-3-octylimidazolium 1,1,1-trifluoro-N-[(trifluoromethyl)sulfonyl]methanesulfonamide	-3,75	210	81
99	61545-99-1	1-Methyl-3-octylimidazolium bromide	-3,93		
100	none (2013-09-19)	1-(11-Ethoxy-11-oxoundecyl)-3-methylimidazolium bromide	-3,93		
101	171058-19-8	1-Methyl-3-octadecylimidazolium chloride	-4,76	242	209
102	244193-52-0	1-Methyl-3-octylimidazolium tetrafluoroborate	-5,32	219	186
103	61546-01-8	1-Hexadecyl-3-methylimidazolium chloride	-5,99	244	220
104	171058-21-2	1-Methyl-3-tetradecylimidazolium chloride	-6,90	245	225

^aIn a list for 245 ILs ordered according to decreasing log(IPC-81) values.

^bIn a list for 232 ILs ordered according to decreasing log(AChE) values.

Table 2: Ranking of ILs according to Bacteria and Fungi toxicity model.

	CAS no.	Name	t[1] Bacteria and Fungi toxicity model
1	126049-85-2	1,3-Bis(propoxymethyl)imidazolium chloride	4,96
2	761410-60-0	1,3-Bis(butoxymethyl)imidazolium chloride	4,81
3	885224-26-0	1-Hexylimidazolium (2S)-2-hydroxypropanoate	4,78
4	615538-92-6	1-Methylimidazolium 2-hydroxypropanoate	4,64
5	1010075-76-9	1-Methylimidazolium (2S)-2-hydroxypropanoate	4,64
6	615538-93-7	1-Ethylimidazolium 2-hydroxypropanoate	4,64
7	none (2013-09-19)	1-Ethylimidazolium (2S)-2-hydroxypropanoate	4,64
8	615538-94-8	1-Propylimidazolium 2-hydroxypropanoate	4,64
9	615538-96-0	1-Pentylimidazolium 2-hydroxypropanoate	4,64
10	none (2013-09-19)	1-Pentylimidazolium (2S)-2-hydroxypropanoate	4,64
11	none (2013-09-19)	1-Propylimidazolium (2S)-2-hydroxypropanoate	4,62
12	885224-25-9	1-Butylimidazolium (2S)-2-hydroxypropanoate	4,54
13	615539-04-3	1-(Butoxymethyl)imidazolium 2-hydroxypropanoate	4,53
14	885224-28-2	1-(Butoxymethyl)imidazolium (2S)-2-hydroxypropanoate	4,53
15	761410-61-1	1,3-Bis[(pentyloxy)methyl]imidazolium chloride	4,47
16	none (2013-09-19)	1-[(Pentyloxy)methyl]imidazolium (2S)-2-hydroxypropanoate	4,34
17	615538-97-1	1-Hexylimidazolium 2-hydroxypropanoate	4,32
18	615539-05-4	1-[(Pentyloxy)methyl]imidazolium 2-hydroxypropanoate	4,11
19	615538-98-2	1-Heptylimidazolium 2-hydroxypropanoate	4,08
20	none (2013-09-19)	1,3-Bis[(tetradecyloxy)methyl]imidazolium chloride	3,76
21	none (2013-09-19)	1,3-Bis[(hexadecyloxy)methyl]imidazolium chloride	3,76
22	885224-29-3	1-[(Hexyloxy)methyl]imidazolium (2S)-2-hydroxypropanoate	3,51
23	none (2013-09-19)	1-Heptylimidazolium (2S)-2-hydroxypropanoate	3,47
24	435346-40-0	3-(Aminocarbonyl)-1-[(cyclododecyloxy)methyl]pyridinium chloride	2,97
25	615539-06-5	1-[(Hexyloxy)methyl]imidazolium 2-hydroxypropanoate	2,87
26	97166-40-0	1-[(Octyloxy)methyl]quinolinium chloride	2,74
27	761410-68-8	1,3-Bis[(dodecyloxy)methyl]imidazolium chloride	2,64
28	97166-39-7	1-[(Hexyloxy)methyl]quinolinium chloride	2,52
29	615539-07-6	1-[(Heptyloxy)methyl]imidazolium 2-hydroxypropanoate	1,94
30	13501-50-3	1-[(Decyloxy)methyl]quinolinium chloride	1,87
31	761410-67-7	1,3-Bis[(undecyloxy)methyl]imidazolium chloride	1,57
32	none (2013-09-19)	1-[(Heptyloxy)methyl]imidazolium (2S)-2-hydroxypropanoate	1,36
33	898558-87-7	1-Octylimidazolium (2S)-2-hydroxypropanoate	1,31
34	41063-22-3	1-[(Dodecyloxy)methyl]quinolinium chloride	1,28

35	435346-42-2	3-(Aminocarbonyl)-1-[(dodecyloxy)methyl]pyridinium iodide	0,91
36	435346-66-0	3-[[[(Decyloxy)methoxy]methyl]amino]carbonyl]-1-[(decyloxy)methyl]pyridinium chloride	0,82
37	615538-99-3	1-Octylimidazolium 2-hydroxypropanoate	0,76
38	435346-76-2	4-(Aminocarbonyl)-1-[(decyloxy)methyl]pyridinium chloride	0,48
39	435346-52-4	3-(Aminocarbonyl)-1-[(dodecyloxy)methyl]pyridinium tetrafluoroborate	0,29
40	97166-41-1	1-[(Hexyloxy)methyl]-6-methylquinolinium chloride	0,25
41	435346-34-2	3-(Aminocarbonyl)-1-[(decyloxy)methyl]pyridinium chloride	0,10
42	615539-08-7	1-[(Octyloxy)methyl]imidazolium 2-hydroxypropanoate	-0,47
43	761410-62-2	1,3-Bis[(hexyloxy)methyl]imidazolium chloride	-0,52
44	435346-77-3	4-(Aminocarbonyl)-1-[(undecyloxy)methyl]pyridinium chloride	-0,81
45	898558-90-2	1-[(Octyloxy)methyl]imidazolium (2S)-2-hydroxypropanoate	-0,92
46	435346-45-5	3-(Aminocarbonyl)-1-[(dodecyloxy)methyl]pyridinium perchlorate	-0,94
47	615539-10-1	1-[(Decyloxy)methyl]imidazolium 2-hydroxypropanoate	-1,36
48	435346-35-3	3-(Aminocarbonyl)-1-[(undecyloxy)methyl]pyridinium chloride	-1,42
49	435346-36-4	3-(Aminocarbonyl)-1-[(dodecyloxy)methyl]pyridinium chloride	-1,51
50	761410-66-6	1,3-Bis[(decyloxy)methyl]imidazolium chloride	-1,59
51	615539-09-8	1-[(Nonyloxy)methyl]imidazolium 2-hydroxypropanoate	-1,60
52	97166-48-8	1-[(Dodecyloxy)methyl]-8-hydroxyquinolinium chloride	-1,67
53	435346-44-4	3-(Aminocarbonyl)-1-[(dodecyloxy)methyl]pyridinium nitrate	-1,75
54	435346-41-1	3-(Aminocarbonyl)-1-[(dodecyloxy)methyl]pyridinium bromide	-1,97
55	97166-46-6	8-Hydroxy-1-[(octyloxy)methyl]quinolinium chloride	-2,03
56	97166-45-5	1-[(Hexyloxy)methyl]-8-hydroxyquinolinium chloride	-2,24
57	435346-55-7	Bis[3-(aminocarbonyl)-1-[(decyloxy)methyl]pyridinium] (T-4)-tetrachlorocuprate	-2,28
58	435346-53-5	3-(Aminocarbonyl)-1-[(dodecyloxy)methyl]pyridinium acetate	-2,43
59	435346-56-8	Bis[3-(aminocarbonyl)-1-[(decyloxy)methyl]pyridinium] (T-4)-tetrachlorozincate	-2,47
60	97166-42-2	6-Methyl-1-[(octyloxy)methyl]quinolinium chloride	-2,58
61	615539-00-9	1-Nonylimidazolium 2-hydroxypropanoate	-2,61
62	435346-58-0	3-(Aminocarbonyl)-1-[(decyloxy)methyl]pyridinium (T-4)-tetrachloroferrate	-2,69
63	898558-88-8	1-Nonylimidazolium (2S)-2-hydroxypropanoate	-2,91
64	615539-12-3	1-[(Dodecyloxy)methyl]imidazolium 2-hydroxypropanoate	-3,14
65	435346-78-4	4-(Aminocarbonyl)-1-[(dodecyloxy)methyl]pyridinium chloride	-3,34
66	435346-54-6	Bis[3-(aminocarbonyl)-1-[(decyloxy)methyl]pyridinium] (T-4)-tetrachlorocobaltate	-3,38
67	898558-91-3	1-[(Nonyloxy)methyl]imidazolium (2S)-2-hydroxypropanoate	-3,51
68	97166-47-7	1-[(Decyloxy)methyl]-8-hydroxyquinolinium chloride	-3,52
69	97166-44-4	1-[(Dodecyloxy)methyl]-6-methylquinolinium chloride	-3,52
70	615539-11-2	1-[(Undecyloxy)methyl]imidazolium 2-hydroxypropanoate	-3,66
71	435346-57-9	Bis[3-(aminocarbonyl)-1-[(decyloxy)methyl]pyridinium] (T-4)-tetrachloromagnesate	-4,18
72	615539-03-2	1-Dodecylimidazolium 2-hydroxypropanoate	-4,31
73	435346-65-9	3-[[[(Nonyloxy)methoxy]methyl]amino]carbonyl]-1-[(nonyloxy)methyl]pyridinium chloride	-4,41
74	435346-63-7	3-[[[(Heptyloxy)methoxy]methyl]amino]carbonyl]-1-[(heptyloxy)methyl]pyridinium chloride	-4,53

75	615539-01-0	1-Decylimidazolium 2-hydroxypropanoate	-4,69
76	615539-02-1	1-Undecylimidazolium 2-hydroxypropanoate	-4,74
77	885224-30-6	1-[(Decyloxy)methyl]imidazolium (2S)-2-hydroxypropanoate	-5,14
78	435346-64-8	3-[[[(Octyloxy)methoxy]methyl]amino]carbonyl]-1-[(octyloxy)methyl]pyridinium chloride	-5,44
79	898558-92-4	1-[(Dodecyloxy)methyl]imidazolium (2S)-2-hydroxypropanoate	-5,81
80	761410-65-5	1,3-Bis[(nonyloxy)methyl]imidazolium chloride	-5,82
81	898223-27-3	1-Decylimidazolium (2S)-2-hydroxypropanoate	-5,89
82	none (2013-09-19)	1-[(Undecyloxy)methyl]imidazolium (2S)-2-hydroxypropanoate	-5,90
83	761410-64-4	1,3-Bis[(octyloxy)methyl]imidazolium chloride	-5,92
84	97166-43-3	1-[(Decyloxy)methyl]-6-methylquinolinium chloride	-6,04
85	761410-63-3	1,3-Bis[(heptyloxy)methyl]imidazolium chloride	-6,54
86	885224-27-1	1-Undecylimidazolium (2S)-2-hydroxypropanoate	-6,93
87	898558-89-9	1-Dodecylimidazolium (2S)-2-hydroxypropanoate	-7,03

Figure Captions

Fig. 1: PCA Scores Plot in the Overall toxicity model

Fig. 2: PCA Loadings Plot in the Overall toxicity model.

Ca 2: *Candida albicans* ATCC 10231 (growth inhib.) 48h;
 Ca 5: *Candida albicans* ATCC 10231 (death) 5d;
 Eh 24: *Enterococcus hirae* ATCC 10541 (growth inhib.) 24h;
 Eh 48: *Enterococcus hirae* ATCC 10541 (death) 48h;
 Ec 24: *Escherichia coli* ATCC 25922 (growth inhib.) 24h;
 Ec 48: *Escherichia coli* ATCC 25922 (death) 48h;
 Kp 24: *Klebsiella pneumoniae* ATCC 4352 (growth inhib.) 24h;
 Kp 48: *Klebsiella pneumoniae* ATCC 4352 (death) 48h;
 Lm fa 7: *Lemna minor* (frond area) 7d;
 Lm fn 7: *Lemna minor* (frond number) 7d;
 Ml 24: *Micrococcus luteus* ATCC 9341 (growth inhib.) 24h;
 Ml 48: *Micrococcus luteus* ATCC 9341 (death) 48h;
 Pv 24: *Proteus vulgaris* NCTC 4635 (growth inhib.) 24h;
 Pv 48: *Proteus vulgaris* NCTC 4635 (death) 48h;
 Pa A 24: *Pseudomonas aeruginosa* ATCC 27853 (growth inhib.) 24h;
 Pa A 48: *Pseudomonas aeruginosa* ATCC 27853 (death) 48h;
 Pa N 24: *Pseudomonas aeruginosa* NCTC 6749 (growth inhib.) 24h;
 Rr 2: *Rhodotorula rubra* PhB (growth inhib.) 48h;

Rr 5: *Rhodotorula rubra* PhB (death) 5d;
 Sv 24: *Scenedesmus vacuolatus* (cell count) 24h;
 Sm 24: *Serratia marcescens* ATCC 8100 (growth inhib.) 24h;
 Sm 48: *Serratia marcescens* ATCC 8100 (death) 48h;
 Sa A 24: *Staphylococcus aureus* ATCC 6538 (growth inhib.) 24h;
 Sa A 48: *Staphylococcus aureus* ATCC 6538 (death) 48h;
 Sa M 24: *Staphylococcus aureus* (MRSA) (growth inhib.) 24h;
 Sa M 48: *Staphylococcus aureus* (MRSA) (death) 48h;
 Sa N 24: *Staphylococcus aureus* NCTC 4163 (growth inhib.) 24h;
 Se 24: *Staphylococcus epidermidis* ATCC 12228 (growth inhib.) 24h;
 Se 48: *Staphylococcus epidermidis* ATCC 12228 (death) 48h;
 Vf 5': *Vibrio fischeri* 5min;
 Vf 15': *Vibrio fischeri* 15min;
 Vf 30': *Vibrio fischeri* 30min;
 AChE: Acetylcholinesterase inhibition;
 IPC-81: IPC-81 leukemia cells cytotoxicity;
 BOD 28: BOD 28d.

Fig. 3: PCA Loadings Plot in the Aquatic toxicity model.

Lm fa 7: *Lemna minor* (frond area) 7d;
 Lm fn 7: *Lemna minor* (frond number) 7d;
 Sv 24: *Scenedesmus vacuolatus* (cell count) 24h;
 Vf 5': *Vibrio fischeri* 5min;
 Vf 15': *Vibrio fischeri* 15min;
 Vf 30': *Vibrio fischeri* 30min.

Fig. 4: PCA Scores Plot in the Aquatic toxicity model.

Fig. 5: PCA Loadings Plot in the Bacteria and Fungi toxicity model.

Ca 2: *Candida albicans* ATCC 10231 (growth inhib.) 48h;
 Ca 5: *Candida albicans* ATCC 10231 (death) 5d;
 Eh 24: *Enterococcus hirae* ATCC 10541 (growth inhib.) 24h;
 Eh 48: *Enterococcus hirae* ATCC 10541 (death) 48h;
 Ec 24: *Escherichia coli* ATCC 25922 (growth inhib.) 24h;
 Ec 48: *Escherichia coli* ATCC 25922 (death) 48h;
 Kp 24: *Klebsiella pneumoniae* ATCC 4352 (growth inhib.) 24h;
 Kp 48: *Klebsiella pneumoniae* ATCC 4352 (death) 48h;
 Ml 24: *Micrococcus luteus* ATCC 9341 (growth inhib.) 24h;
 Ml 48: *Micrococcus luteus* ATCC 9341 (death) 48h;
 Pv 24: *Proteus vulgaris* NCTC 4635 (growth inhib.) 24h;
 Pv 48: *Proteus vulgaris* NCTC 4635 (death) 48h;
 Pa A 24: *Pseudomonas aeruginosa* ATCC 27853 (growth inhib.) 24h;

Pa A 48: *Pseudomonas aeruginosa* ATCC 27853 (death) 48h;
 Pa N 24: *Pseudomonas aeruginosa* NCTC 6749 (growth inhib.) 24h;
 Rr 2: *Rhodotorula rubra* PhB (growth inhib.) 48h;
 Rr 5: *Rhodotorula rubra* PhB (death) 5d;
 Sm 24: *Serratia marcescens* ATCC 8100 (growth inhib.) 24h;
 Sm 48: *Serratia marcescens* ATCC 8100 (death) 48h;
 Sa A 24: *Staphylococcus aureus* ATCC 6538 (growth inhib.) 24h;
 Sa A 48: *Staphylococcus aureus* ATCC 6538 (death) 48h;
 Sa M 24: *Staphylococcus aureus* (MRSA) (growth inhib.) 24h;
 Sa M 48: *Staphylococcus aureus* (MRSA) (death) 48h;
 Sa N 24: *Staphylococcus aureus* NCTC 4163 (growth inhib.) 24h;
 Se 24: *Staphylococcus epidermidis* ATCC 12228 (growth inhib.) 24h;
 Se 48: *Staphylococcus epidermidis* ATCC 12228 (death) 48h.

Fig. 6: PCA Scores Plot in the Bacteria and Fungi toxicity model.

Fig. 7: PCA Scores Plot in the Overall toxicity model for imidazolium-based ILs.

Fig. 8: PCA-class Scores Plot in the Overall toxicity model for imidazolium chloride-based ILs.

Fig. 9: PCA-class Loadings Plot in the Overall toxicity model for imidazolium chloride-based ILs.

Ca 2: *Candida albicans* ATCC 10231 (growth inhib.) 48h;
 Ca 5: *Candida albicans* ATCC 10231 (death) 5d;
 Eh 24: *Enterococcus hirae* ATCC 10541 (growth inhib.) 24h;
 Eh 48: *Enterococcus hirae* ATCC 10541 (death) 48h;
 Eh D 48: *Enterococcus hirae* DSM 20160 (death) 48h;
 Ec 24: *Escherichia coli* ATCC 25922 (growth inhib.) 24h;
 Ec 48: *Escherichia coli* ATCC 25922 (death) 48h;
 Kp 24: *Klebsiella pneumoniae* ATCC 4352 (growth inhib.) 24h;
 Kp 48: *Klebsiella pneumoniae* ATCC 4352 (death) 48h;
 Kp A 48h: *Klebsiella pneumoniae* ATCC 13886 (death) 48h;
 Lm fa 7: *Lemna minor* (frond area) 7d;
 Lm fn 7: *Lemna minor* (frond number) 7d;
 Ml 24: *Micrococcus luteus* ATCC 9341 (growth inhib.) 24h;
 Ml 48: *Micrococcus luteus* ATCC 9341 (death) 48h;
 Pv 24: *Proteus vulgaris* NCTC 4635 (growth inhib.) 24h;

Pv 48: *Proteus vulgaris* NCTC 4635 (death) 48h;
 Pa A 24: *Pseudomonas aeruginosa* ATCC 27853 (growth inhib.) 24h;
 Pa A 48: *Pseudomonas aeruginosa* ATCC 27853 (death) 48h;
 Rrb 5: *Rhodotorula rubra* (death) 5d;
 Rr 2: *Rhodotorula rubra* PhB (growth inhib.) 48h;
 Rr 5: *Rhodotorula rubra* PhB (death) 5d;
 Sv 24: *Scenedesmus vacuolatus* (cell count) 24h;
 Sm 24h: *Serratia marcescens* ATCC 8100 (growth inhib.) 24h;
 Sm 48: *Serratia marcescens* ATCC 8100 (death) 48h;
 Sa A 24: *Staphylococcus aureus* ATCC 6538 (growth inhib.) 24h;
 Sa A 48: *Staphylococcus aureus* ATCC 6538 (death) 48h;
 Sa M 24: *Staphylococcus aureus* (MRSA) (growth inhib.) 24h;
 Sa M 48: *Staphylococcus aureus* (MRSA) (death) 48h;
 Sa MA 48: *Staphylococcus aureus* (MRSA) ATCC 43300 (death) 48h;
 Se 24: *Staphylococcus epidermidis* ATCC 12228 (growth inhib.) 24h;

Se 48: *Staphylococcus epidermidis* ATCC 12228 (death) 48h;
Se N 48: *Staphylococcus epidermidis* NCTC 11047 (death) 48h;
Vf 15': *Vibrio fischeri* 15min;

Vf 30': *Vibrio fischeri* 30min;
AChE: Acetylcholinesterase inhibition;
IPC-81: IPC-81 leukemia cells cytotoxicity.

Fig. 10 Correlations among different toxicities.

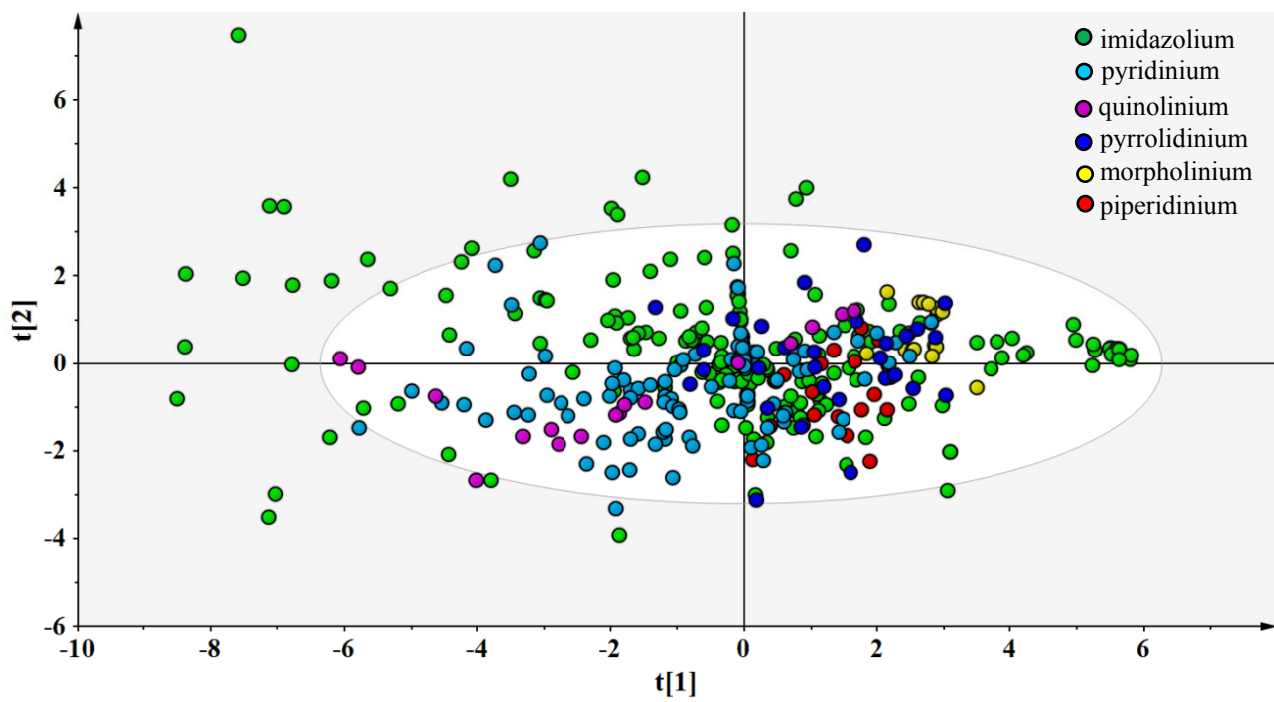


Figure 1

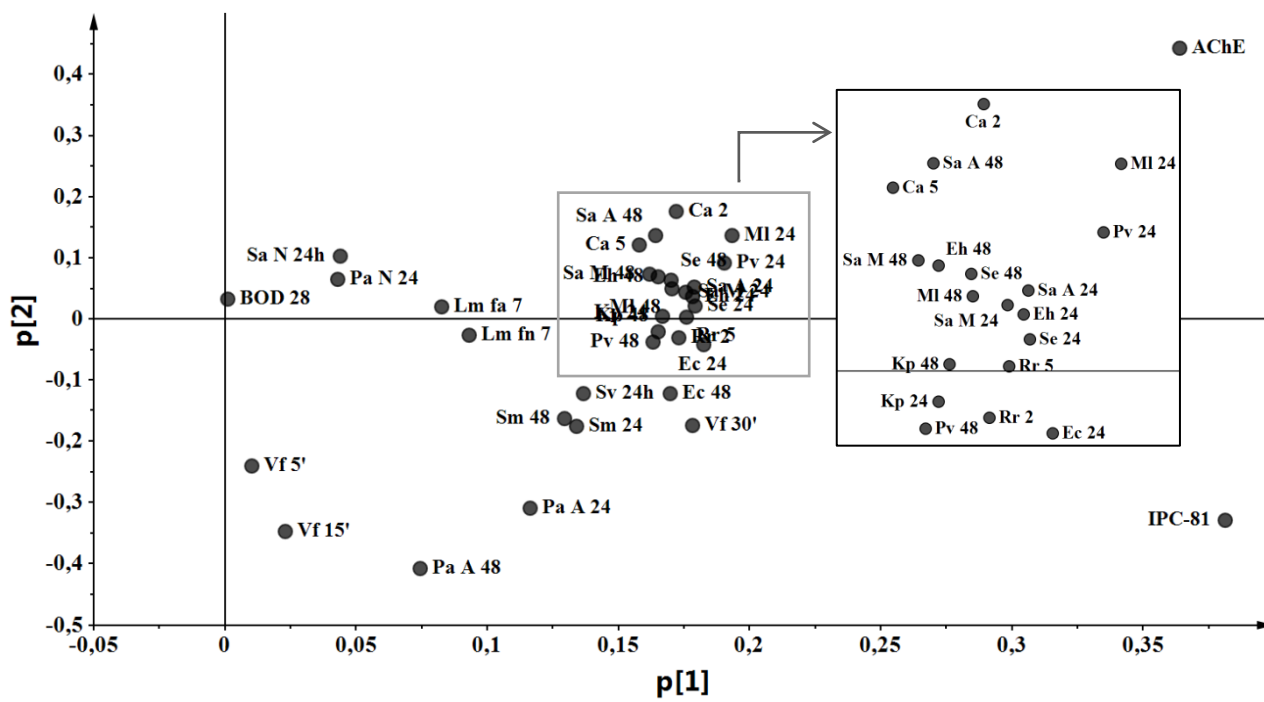


Figure 2

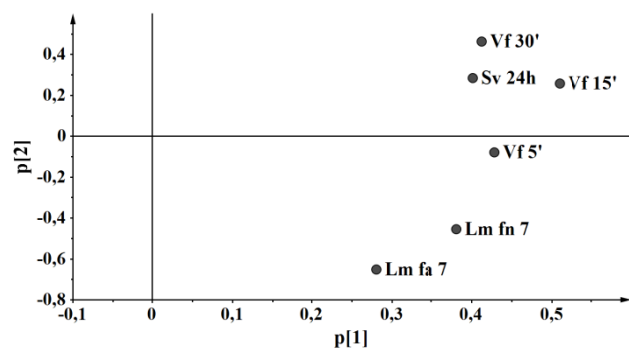


Figure 3

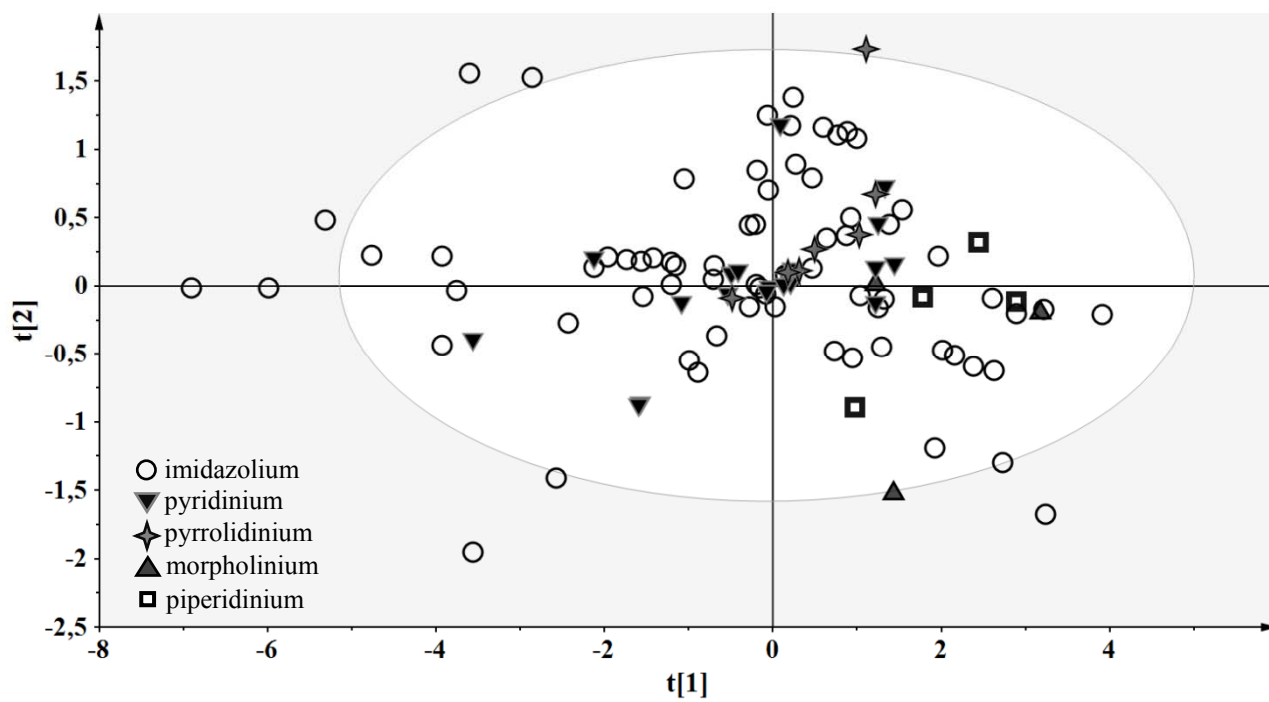


Figure 4

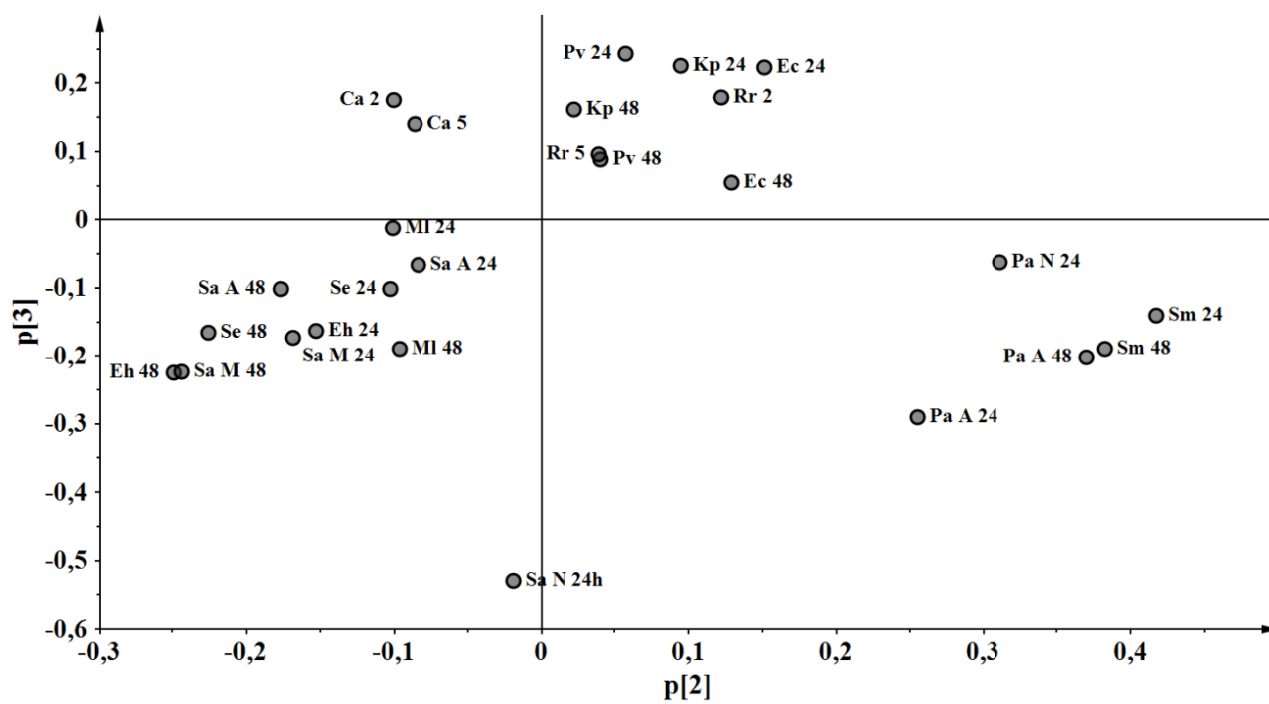


Figure 5

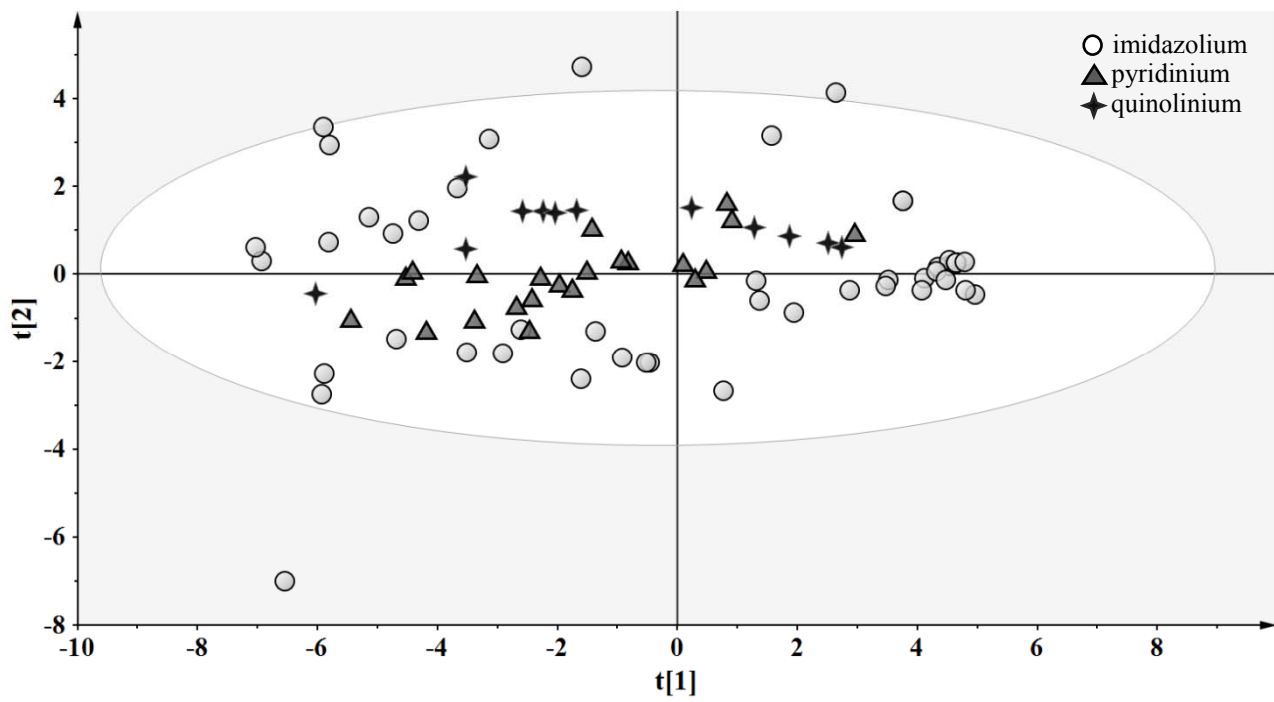


Figure 6

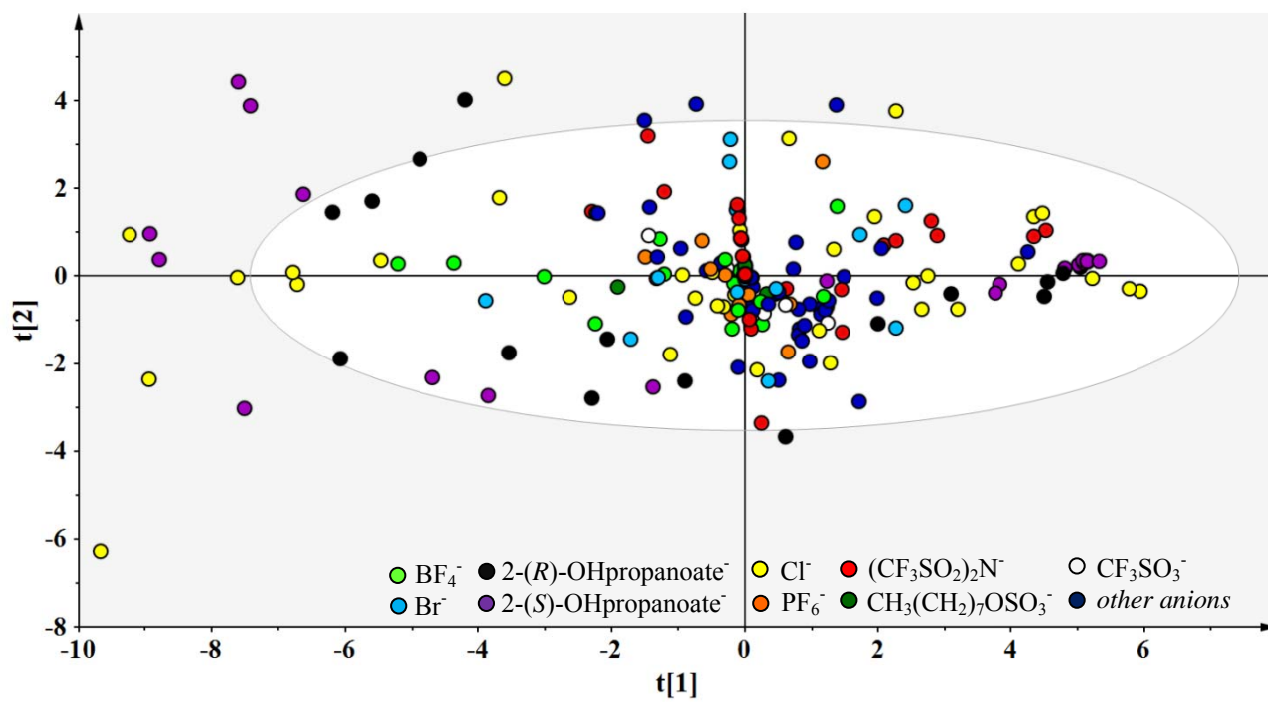


Figure 7

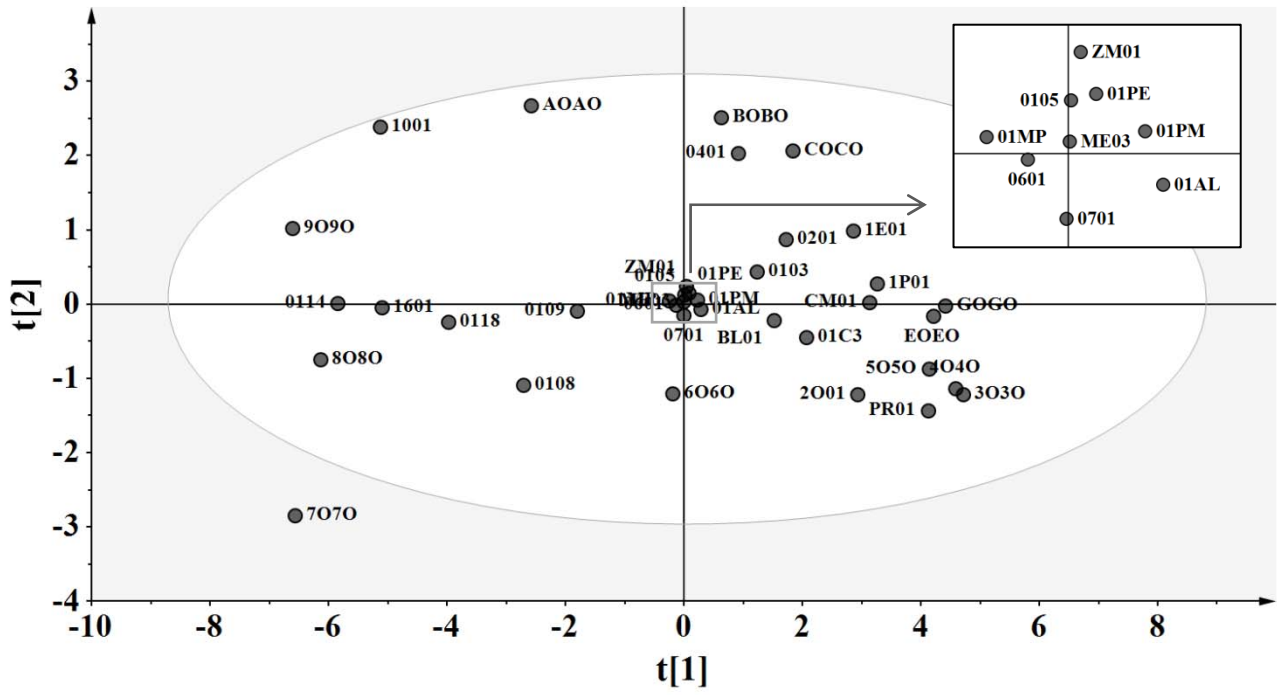


Figure 8

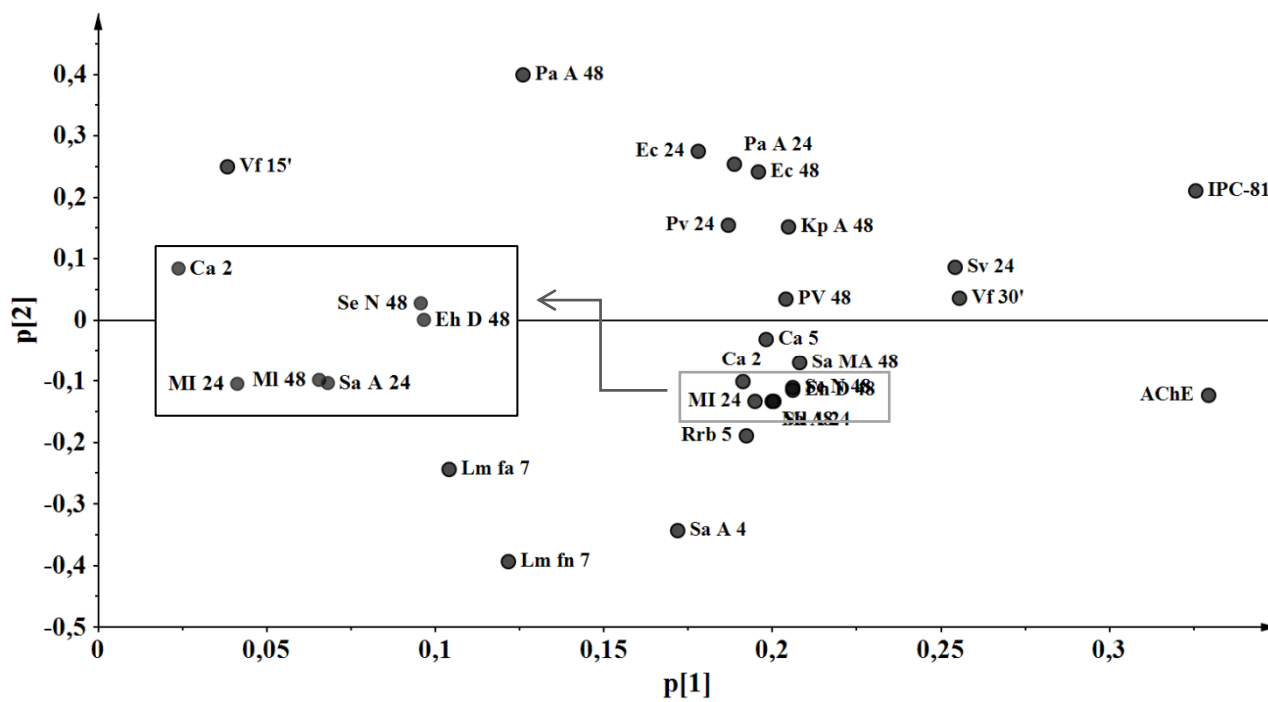


Figure 9

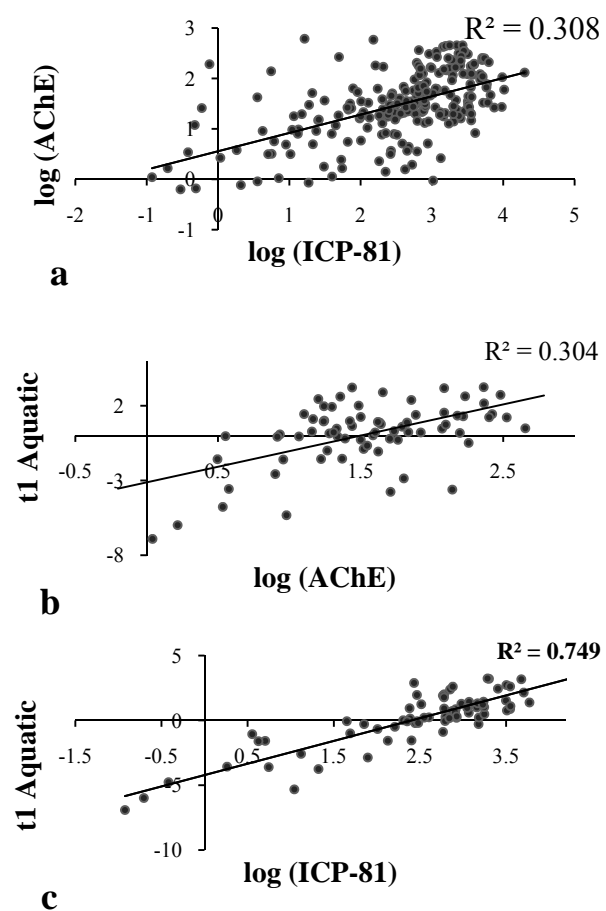


Figure 10